Bioorganic Chemistry 93 (2019) 103309

Contents lists available at ScienceDirect

Bioorganic Chemistry

journal homepage: www.elsevier.com/locate/bioorg

Discovery of novel oxoindolin derivatives as atypical dual inhibitors for DNA Gyrase and FabH

Yu-Shun Yang[a,1,*], Mi-Mi Su[a,1], Jian-Fei Xu[a], Qi-Xing Liu[a], Li-Fei Bai[c], Xiao-Wei Hu[b,*], Hai-Liang Zhu[a,*]

[a] State Key Laboratory of Pharmaceutical Biotechnology, Nanjing University, Nanjing 210023, China
[b] School of Chemistry and Chemical Engineering, Linyi University, Linyi, Shandong 276005, China
[c] Jiangsu Key Laboratory of Bio-function Molecule, College of Life Science and Chemistry & Chemical Engineering, Jiangsu Second Normal University, Nanjing 210013, China

ARTICLE INFO

Keywords:
Antimicrobial
Atypical dual inhibitor
DNA Gyrase
FabH
Molecular docking
3D QSAR

ABSTRACT

The antibacterial agents and therapies today are facing serious problems such as drug resistance. Introducing dual inhibiting effect is a valid approach to solve this trouble and bring advantages including wide adaptability, favorable safety and superiority of combination. We started from potential DNA Gyrase inhibitory backbone isatin to develop oxoindolin derivatives as atypical dual Gyrase (major) and FabH (assistant) inhibitors via a two-round screening. Aiming at blocking both duplication (Gyrase) and survival (FabH), most of synthesized compounds indicated potency against Gyrase and some of them inferred favorable inhibitory effect on FabH. The top hit **I18** suggested comparable Gyrase inhibitory activity (IC_{50} = 0.025 μM) and antibacterial effect with the positive control Novobiocin (IC_{50} = 0.040 μM). FabH inhibitory activity (IC_{50} = 5.20 μM) was also successfully introduced. Docking simulation hinted possible important interacted residues and binding patterns for both target proteins. Adequate Structure-Activity Relation discussions provide the future orientations of modification. With high potency, low initial toxicity and dual inhibiting strategy, advanced compounds with therapeutic methods will be developed for clinical application.

1. Introduction

The antibacterial agents and therapies today are facing serious problems such as drug resistance [1,2]. The abuse of antibiotics has aggravated the unfavorable situation [3,4]. Novel functional molecules with potential antibacterial potency are in urgent need to bring new hope in curing bacterial infections and diseases [5–8]. Meanwhile, introducing dual inhibiting effect is reported as a valid approach to solve this trouble [9–12]. Usually, dual inhibiting has advantages including wide adaptability, favorable safety and superiority of combination [13–16]. When mono-targeting strategy limited researchers within the dilemma of balancing the potency with toxicity and the threat of more easily causing drug-resistance, typical dual-targeting strategy would break the limits [17].

Herein, we investigated two targets, DNA Gyrase (Gyr) [18] and FabH [19]. The former causes negative supercoiling of the DNA or relaxes positive supercoils [20–22]. Due to the structural differences in prokaryotes and eukaryotes, DNA Gyrase is targeted by antibiotics including Ciprofloxacin into subunit A and Novobiocin into subunit B [23]. Mimicing typical DNA Gyrase inhibitors has been reported to be a practical tactic to develop similar prodrugs [24–27]. FabH, also called *β*-ketoacyl-acyl carrier protein synthase III, catalyzes the starting step of bacterial fatty acid synthesis [28–30], an significant process in the metabolism [31,32]. In particular, FabH only exists in bacteria and plants [33]. Our task is achieving dual inhibitors, thus blocking both the duplication and survival of pathogenic bacteria.

In consideration of the inclination for targets in the physiological processes, we used an atypical dual-targeting strategy as reported [34]. DNA Gyrase was regarded as the major target and FabH was set as the assistant one because duplication was more fierce than survival, therefore our choice was developing FabH inhibition upon DNA Gyrase inhibitors. Shown in Fig. 1, we selected isatin as the initial backbone due to the reported cases of its modification for exploiting DNA Gyrase inhibitors [35–38] like its analogous flavonoids [39–42]. After seriously evaluating the similarity of the two subunits of DNA Gyrase via homologous modeling (Fig. S1) and overall *in silico* study, we attempted to use the cyclopropyl moiety, a typical feature of DNA Gyrase

* Corresponding authors.
E-mail addresses: ys_yang@nju.edu.cn (Y.-S. Yang), hxwfly2009@163.com (X.-W. Hu), zhuhl@nju.edu.cn (H.-L. Zhu).
[1] Both authors contributed equally to the work.

https://doi.org/10.1016/j.bioorg.2019.103309
Received 30 July 2019; Received in revised form 20 August 2019; Accepted 19 September 2019
Available online 21 September 2019
0045-2068/

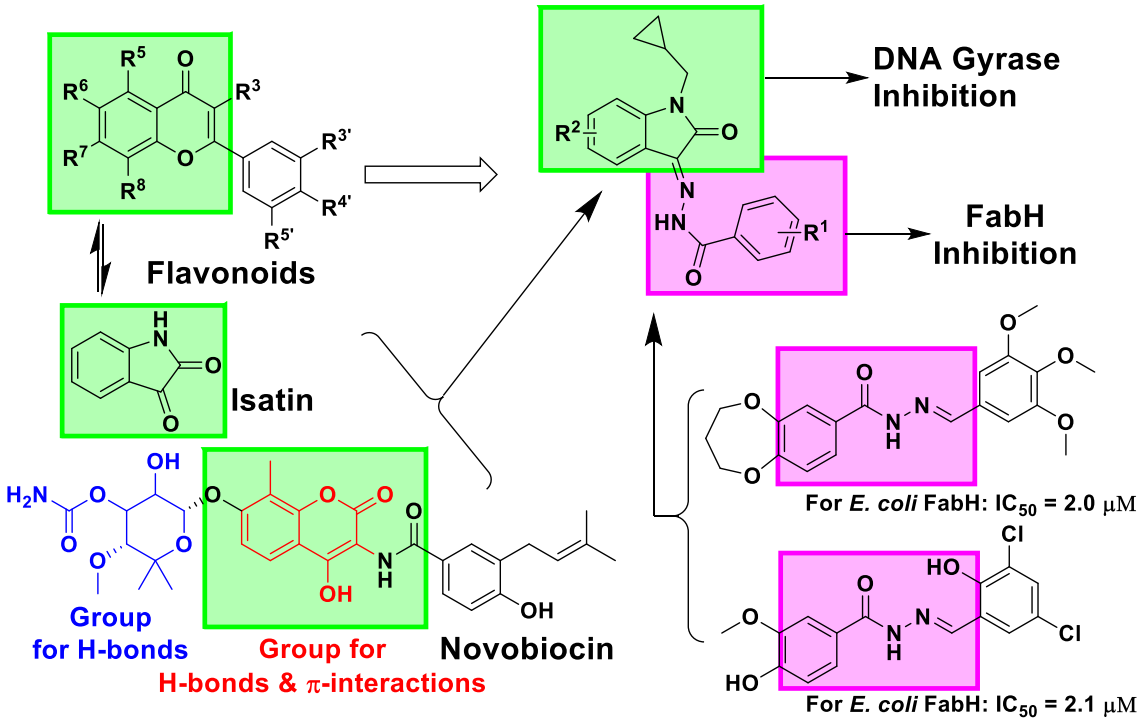

Fig. 1. The designing concept of the dual DNA Gyrase and FabH inhibitors.

inhibitors (usually for GyrA and recently reported for GyrB [43]). Based on Structure-Based Drug Design and bioisosterism, we took the similarity of isatin, flavonoid and Novobiocin (Gyrase inhibitor, IC_{50} = 0.040 μM) to regenerate the backbone with the feasible addition of cyclopropyl. The calculated binding situations suggested inhibitory potential (Supporting Information, SI). For introducing FabH inhibitory potential, none of the reported controls (Thiolactomycin, Platensimycin and Kanamycin B) was suitable for hybridization. Tentatively, we selected the acylhydrazone moiety (−C═N−NH−CO−) because when this pharmacophore was added on alternative backbones [44–47], the potency could be retained to some extent. Fully investigated the feasibility of the new generated series through designing rationale and preliminary docking simulation, we conducted the two-round screening with enriched substitutes. We preferred the top hits as atypical dual inhibitors mainly for Gyrase and auxiliarily for FabH, according to their tendentious functions on duplication and survival.

2. Experimental section

The experimental section with NMR information and spectra were detailed in the Supporting Information.

3. Results and discussion

3.1. Synthesis of the compounds

The oxoindolin derivatives **H1-H20** (H for "hydrazine") and **I1-I30** (I for "isatin") were synthesized in two rounds. All (except **H20**) were reported for the first time with satisfactory analytical and spectroscopic data (SI). No *cis–trans* isomerism was found during reaction, and NMR data indicated all the series were *trans* configuration. The general synthesis method was outlined in Scheme 1. First, substituted isatin was stirred in DMF at 50 °C with (bromomethyl)cyclopropane and K_2CO_3 added, yielding 1-(cyclopropylmethyl)indoline-2,3-dione (**B**). Second, a condensation reaction using hydrazine reagents resulted in the target compounds **H1-H20** and **I1-I30**. The expansion to form **I1-I30** was based on the biological performances of **H1-H20**.

3.2. Biological evaluation and the two-round screening

The synthesized **H1-H20** were evaluated for their Gyrase and FabH inhibitory activities. The results were expressed as IC_{50} (the half maximal inhibitory concentration), presented in Table 1.

Most of this series indicated potency against Gyrase, and some of them inferred favorable inhibitory effect on FabH. Since the Gyrase inhibition seemed in the leading position, a preliminary Structure-Activity Relationship (SAR) discussion on Gyrase inhibition was conducted. Several hints could be inferred. The first hint was that among simple substitutes, putting it on *para*-position was superior to on *meta*-position. All involved substitutes (-F, -Cl, -Br and -OMe) obeyed this hint. The second hint was that multi-substituted ones (**H15-H18**) were potential for inhibition, but not better than the top single-substituted ones (**H5**, ***H10***). Thus we regarded the comparison of simple substitute on *para*-position as the most significant clue. Here the steric effect was more decisive than the electronic affection. The corresponding order (" > " meant "better than") was -Me (IC_{50} = 0.950 μM) > -OPh (IC_{50} = 1.22 μM) > $-CF_3$ (IC_{50} = 10.1 μM) ≥ $-^{i}Pr$ (IC_{50} = 10.4 μM) > -OMe (IC_{50} = 11.8 μM) > -Br (IC_{50} = 12.3 μM) > -Cl (IC_{50} = 13.1 μM) > -F (IC_{50} = 14.8 μM) > -H (IC_{50} = 15.1 μM) > $-^{t}Bu$ (IC_{50} = 24.7 μM). Thus, two choices, providing substitute of suitable size (eg. -Me) or stretching the backbone to outer space (eg. -OPh), were beneficial for modification. In addition, defaulting part of the backbone (**H19**, **H20**) ruined the inhibitory activity.

One step further, we completed the default discussion on oxoindolin. Several single substitutes (-F, -Cl, -Br, -Me) were added on the position of or next to the same one of Novobiocin. According to the SAR discussion of **H** series, simple *para*-substituted ring was selected for this step. Then the subsequent **I** series were generated with the tested results in Table 2.

Most of the expanded compounds inferred improved Gyrase inhibitory activity and some of them retained potency against FabH. The added factor made the SAR on Gyrase more complex. For the benzene substitute R^1, the original order in **H** series was -Me > -OPh > -Br > -Cl > -F > -H, and the basic tendency in **I** series was almost the same. When we divided **I** series by the oxoindolin substitute R^2 and discussed R^1, -Me and -OPh occupied two of the top three in each

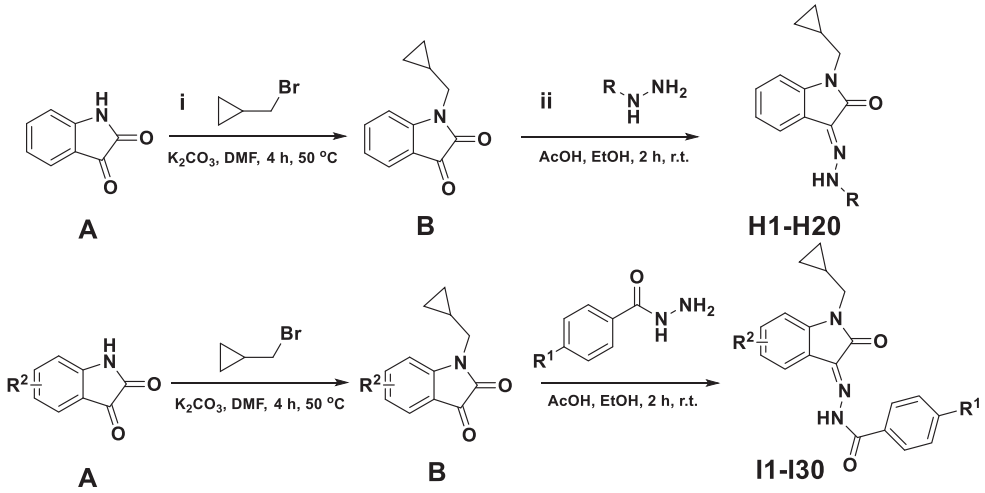

Code	R	Code	R
H1	Benzoyl	**H11**	3- Fluorobenzoyl
H2	4-Fluorobenzoyl	**H12**	3-Chlorobenzoyl
H3	4-Chlorobenzoyl	**H13**	3-Bromobenzoyl
H4	4-Bromobenzoyl	**H14**	3-Methoxybenzoyl
H5	4-Methylbenzoyl	**H15**	3-Fluoro-4-methoxybenzoyl
H6	4-Methoxybenzoyl	**H16**	3,4-Dimethoxybenzoyl
H7	4-Isopropylbenzoyl	**H17**	3,5-Dimethylbenzoyl
H8	4-Tert-butylbenzoyl	**H18**	3,5-Dimethoxybenzoyl
H9	4-Trifluoromethylbenzoyl	**H19**	Phenyl
H10	4-Phenyloxybenzoyl	**H20**	Thiocarbamoyl

Code	R^1	R^2	Code	R^1	R^2	Code	R^1	R^2
I1	-H	5-F	**I11**	-Me	5-Cl	**I21**	-Cl	4-Br
I2	-F	5-F	**I12**	-OPh	5-Cl	**I22**	-Br	4-Br
I3	-Cl	5-F	**I13**	-H	5-Br	**I23**	-Me	4-Br
I4	-Br	5-F	**I14**	-F	5-Br	**I24**	-OPh	4-Br
I5	-Me	5-F	**I15**	-Cl	5-Br	**I25**	-H	5-Me
I6	-OPh	5-F	**I16**	-Br	5-Br	**I26**	-F	5-Me
I7	-H	5-Cl	**I17**	-Me	5-Br	**I27**	-Cl	5-Me
I8	-F	5-Cl	**I18**	-OPh	5-Br	**I28**	-Br	5-Me
I9	-Cl	5-Cl	**I19**	-H	4-Br	**I29**	-Me	5-Me
I10	-Br	5-Cl	**I20**	-F	4-Br	**I30**	-OPh	5-Me

Scheme 1. The general synthesis and structures of compounds **H1-H20** and **I1-I30**.

division while -H was always the bottom one. When discussing oxoindolin substitute R^2, we could get two hints. One was that the steric affection was still decisive, with the approximate order of -Cl (**I7-I12**) > -Me (**I25-I30**) > -Br (**I13-I18**) > -F (**I1-I6**). The other was that if we moved the position (from 5- to 4-) of the substitute, the affection of different substitutes showed less fluctuation while the top one

Table 1
DNA Gyrase and FabH inhibitory activities of **H1-H20**.

Code	IC_{50} (μM)Gyrase	IC_{50} (μM)FabH	Code	IC_{50} (μM)Gyrase	IC_{50} (μM)FabH
H1	15.1 ± 1.15	15.2 ± 1.37	**H11**	35.8 ± 3.22	N.D.
H2	14.8 ± 1.23	N.D.	**H12**	20.2 ± 1.83	N.D.
H3	13.1 ± 1.07	10.8 ± 1.01	**H13**	55.7 ± 4.75	N.D.
H4	12.3 ± 1.03	N.D.	**H14**	17.2 ± 1.31	146 ± 12.1
H5	0.950 ± 0.080	10.6 ± 1.00	**H15**	5.95 ± 0.48	N.D.
H6	11.8 ± 1.02	3.50 ± 0.32	**H16**	4.43 ± 0.41	N.D.
H7	10.4 ± 1.00	14.5 ± 1.18	**H17**	15.5 ± 1.38	N.D.
H8	24.7 ± 2.06	47.5 ± 4.52	**H18**	1.98 ± 0.15	N.D.
H9	10.1 ± 0.95	15.8 ± 1.35	**H19**	> 200	N.D.
H10	1.22 ± 0.11	21.0 ± 1.96	**H20**	> 200	24.2 ± 2.28
Novobiocin	0.040 ± 0.003	—	Kanamycin B	—	3.15 ± 0.30

N.D. meant Not Detected at highest concentration tested (500 μM).

Table 2
DNA Gyrase and FabH inhibitory activities of **I1-I30**.

Code	IC_{50} (μM)Gyrase	IC_{50} (μM)FabH	Code	IC_{50} (μM)Gyrase	IC_{50} (μM)FabH
I1	78.2 ± 7.51	N.D.	**I16**	26.3 ± 2.45	N.D.
I2	38.9 ± 3.68	4.10 ± 0.36	**I17**	2.37 ± 0.21	N.D.
I3	0.19 ± 0.015	N.D.	**I18**	0.025 ± 0.002	5.20 ± 0.51
I4	8.15 ± 0.76	12.4 ± 1.10	**I19**	7.10 ± 0.65	N.D.
I5	6.65 ± 0.63	4.30 ± 0.40	**I20**	4.25 ± 0.40	N.D.
I6	5.28 ± 0.48	2.85 ± 0.23	**I21**	6.47 ± 0.52	18.2 ± 1.59
I7	4.88 ± 0.45	N.D.	**I22**	6.20 ± 0.58	N.D.
I8	2.60 ± 0.23	N.D.	**I23**	4.02 ± 0.35	68.2 ± 6.34
I9	3.42 ± 0.31	N.D.	**I24**	0.480 ± 0.036	102 ± 9.89
I10	2.18 ± 0.20	N.D.	**I25**	113 ± 10.6	N.D.
I11	0.075 ± 0.006	N.D.	**I26**	19.8 ± 1.80	N.D.
I12	0.028 ± 0.002	8.35 ± 0.78	**I27**	12.1 ± 1.14	N.D.
I13	157 ± 14.9	N.D.	**I28**	1.65 ± 0.16	N.D.
I14	1.41 ± 0.12	N.D.	**I29**	2.49 ± 0.22	N.D.
I15	41.6 ± 3.70	N.D.	**I30**	0.031 ± 0.003	7.10 ± 0.69
Novobiocin	0.040 ± 0.003	—	Kanamycin B	—	3.15 ± 0.30

N.D. meant Not Detected at highest concentration tested (500 μM).

Table 3
Antibacterial and cytotoxic performances of representatives.

Code	MIC (μM)MSSA	MIC (μM)MSSA + Tween80	MIC (μM)MRSA	MIC (μM)QRSA	MIC (μM)*P. aeruginosa*	IC_{50} (μM)293 T
I18	0.15 ± 0.01	0.17 ± 0.01	0.14 ± 0.01	8.25 ± 0.72	1.38 ± 0.12	> 200
I12	0.31 ± 0.03	0.35 ± 0.03	0.30 ± 0.02	12.5 ± 1.05	2.04 ± 0.18	195 ± 16.5
I30	0.42 ± 0.04	0.50 ± 0.04	0.54 ± 0.05	10.2 ± 0.87	2.13 ± 0.20	> 200
I11	1.05 ± 0.09	1.04 ± 0.08	0.98 ± 0.08	150 ± 14.5	2.74 ± 0.25	187 ± 15.2
I3	1.86 ± 0.15	1.91 ± 0.16	2.14 ± 0.19	> 200	3.85 ± 0.35	178 ± 15.6
I24	4.17 ± 0.36	5.26 ± 0.50	7.15 ± 0.68	95.2 ± 7.93	6.25 ± 0.52	> 200
H5	7.58 ± 0.51	8.87 ± 0.78	10.3 ± 0.96	18.3 ± 1.70	8.36 ± 0.78	> 200
H10	10.2 ± 0.84	12.9 ± 1.12	9.16 ± 0.82	25.2 ± 2.15	9.26 ± 0.83	> 200
H19	> 200	> 200	> 200	> 200	75.7 ± 7.31	158 ± 14.8
I13	> 200	> 200	> 200	> 200	52.8 ± 5.10	> 200
Novobiocin	0.79 ± 0.07	0.78 ± 0.07	0.85 ± 0.06	38.5 ± 2.75	48.5 ± 4.3	> 200

was less potent (**I19-I24** vs. **I13-I18**). Fortunately, after this round, the top ones were comparable with the positive control on DNA Gyrase inhibition. Since the SAR of Gyrase inhibition was not concise enough and that of FabH was difficult to be induced in independent series, visualized SARs of both targets were displayed in the 3D QSAR part.

We chose the top 8 and bottom 2 (one for each round) compounds in Gyrase inhibition screening to evaluate their antibacterial and cytotoxic performances. Tween80 was used to eliminate the impact of blocking fatty acid synthesis, thus to weaken the impact of FabH inhibition [48]. As seen in Table 3, the selected compounds all suggested favorable antibacterial activity and low toxicity. Noticeably, they did not show remarkable potency against quinolone-resistant *Staphylococcus aureus* (QRSA, resistant to both GyrA and GyrB inhibitors) [49], indicating that their effect was mainly based on DNA Gyrase inhibition. Meanwhile, FabH inhibition could retain some potency against bacteria when Gyrase inhibition was blocked.

Flow cytometry analysis was conducted to indicate the antibacterial activity on *S. aureus*. As shown in Fig. 2, when we treated the bacteria with increasing concentrations of **I18** (0–0.50 μM) for 48 h, the percentage of apoptotic cocci displayed a significant increase in a dose-dependent manner. This result agreed with that of MTT method.

3.3. In silico study

For *in silico* study (detailed in SI), the ADMET simulation indicated that almost all the compounds suggested good potential in druggability. Along with the modification, the molecular docking models hinted possible binding situations. For Gyrase, key residues included Asp81, Arg84, Gly85, Arg144 and Thr173, which basically agreed with precious models; while for FabH, key residues included Met201, His238,

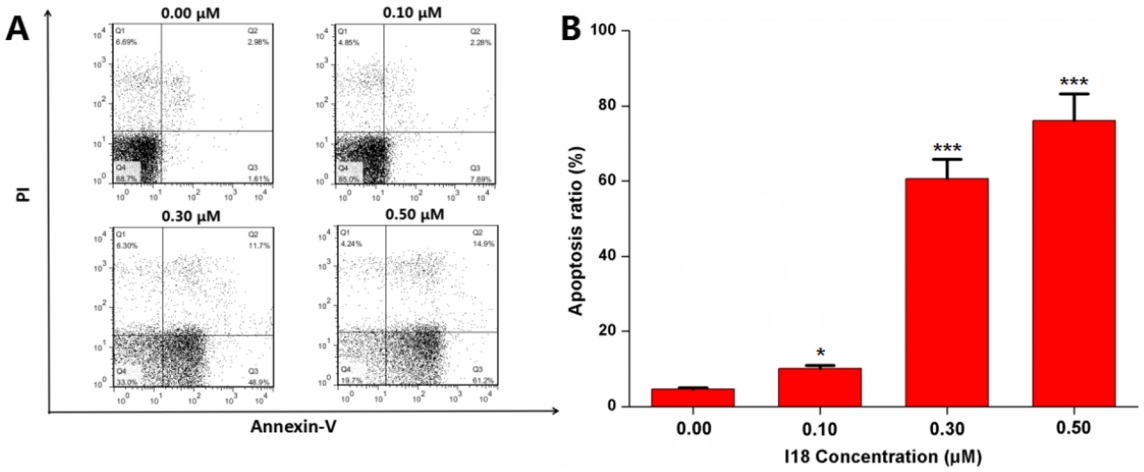

Fig. 2. Flow cytometry analysis of **I18** on *S. aureus*. The dose-dependent apoptosis for 48 h.

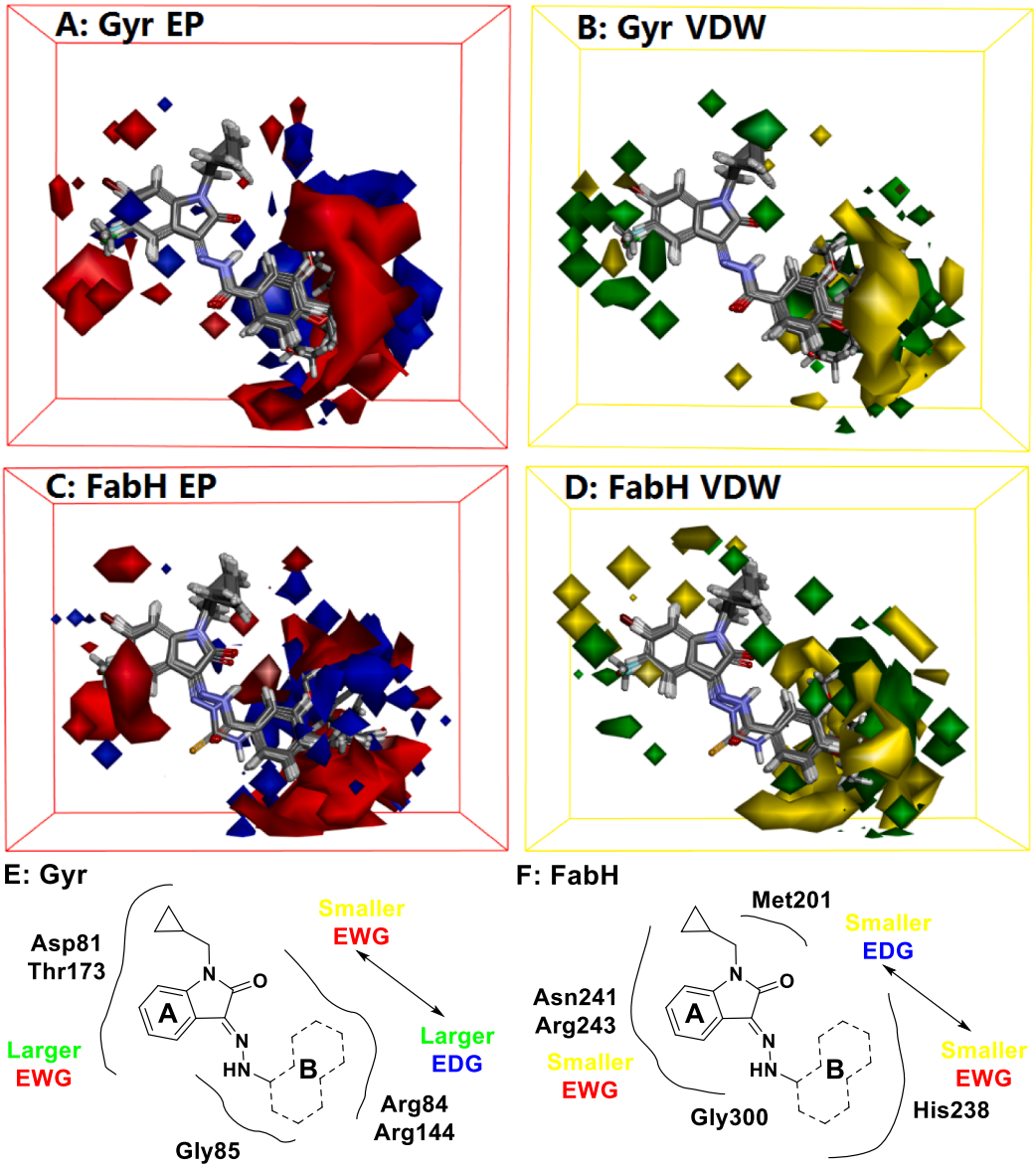

Fig. 3. 3D-QSAR models of selected compounds into Gyrase and FabH. The maps of electronic potential (A & C), *Van der Waals* grids (B & D) and brief illustrations (E & F) visualized the requirements of each factor.

Asn241, Arg243 and Gly300.

To provide more brief SAR discussion, 3D QSAR models were built. For Gyrase we took the top 40 compounds (conventional largest sample size) while for FabH we took all the 20 compounds with correlated activity. 80% of the compounds were chosen by random as training sets while the rest 20% (**H5, H8, *H*10, H17, I17, I18, I20, I21** for Gyrase; **H7, *H*10, H20, I12** for FabH) were defined as test sets. The correlation coefficient r^2 (0.856 for Gyrase; 0.967 for FabH) guaranteed the reliability of both the models ($r^2 > 0.400$). The maps of electronic potential (red for electronic withdrawing in need while blue for electronic donating) and *Van der Waals* grids (green for bulky group in need while yellow for smaller) were shown in Fig. 3. For Gyrase, the modification on the oxoindolin moiety required bulky electronic-withdrawing substitutes. On the introduced benzene ring, smaller electronic-withdrawing group was needed in the nearby region whereas larger electronic-donating one was suitable in the outer-stretched region. This result agreed with the preliminary Structure-Activity Relationship discussion upon the substitutes. For FabH, smaller backbone was a basic requirement all around. Although electronic-withdrawing group seemed better on both modified sites, an electronic-donating one was still acceptable along the nearer *meta*-position of the introduced benzene ring.

4. Conclusion

In summary, this work performed a two-round screening of oxoindolin derivatives as dual DNA Gyrase and FabH inhibitors. It combined the procedures of modification, biological evaluation and *in silico* study. From potential DNA Gyrase inhibitory backbone isatin, we improved the Gyrase inhibition effect and introduced the possibility as FabH inhibitors to realize the blocking of both duplication and survival. Most of both series indicated potency against Gyrase and some of them inferred favorable inhibitory effect on FabH. The top hit **I18** suggested comparable Gyrase inhibitory activity ($IC_{50} = 0.025\,\mu M$) and antibacterial effect with the positive control Novobiocin ($IC_{50} = 0.040\,\mu M$). It also possessed FabH inhibitory activity ($IC_{50} = 5.20\,\mu M$) which enhanced its potential of atypically inhibiting dual targets and fighting drug-resistance. Docking simulation provided the possible binding pattern into both Gyrase and FabH, which picked probable important interacted residues (Asp81, Arg84, Gly85, Arg144, Thr173 of Gyrase and Met201, His238, Asn241, Arg243, Gly300 of FabH). 3D-QSAR models and the substitute-based discussion hinted the future modification of controlling the size of the whole molecule with electron-withdrawing surrounding but jumping out to introduce electron-donating periphery. On the basis of high potency, low initial toxicity and dual inhibiting strategy, further studies will be performed to identify advanced molecules with therapeutic approaches and clinical potential.

Acknowledgements

This work is supported by the Fundamental Research Funds for the Central Universities, China (No. 020814380063), Shandong Provincial Natural Science Foundation, China (No. ZR2018LB004), Natural Science Foundation of the Jiangsu Higher Education Institutions of China (No. 15KJA350001), the National Undergraduate Innovation Program and the National Science Foundation of China (No. J1210026).

Declaration of Competing Interest

The authors have no conflict of interests to declare.

Appendix A. Supplementary material

In silico study, experimental section, detailed NMR information and spectra were detailed in the Supporting Information. Supplementary data to this article can be found online at https://doi.org/10.1016/j.bioorg.2019.103309.

References

[1] N. Wale, D.G. Sim, M.J. Jones, R. Salathe, T. Day, A.F. Read, Resource limitation prevents the emergence of drug resistance by intensifying within-host competition, Proc. Natl. Acad. Sci. U.S.A. 114 (2017) 13774–13779.
[2] R.D. Ducati, H.A. Namanja-Magliano, R.K. Harijan, J.E. Fajardo, A. Fiser, J.P. Daily, V.L. Schramm, Genetic resistance to purine nucleoside phosphorylase inhibition in *Plasmodium falciparum*, Proc. Natl. Acad. Sci. U.S.A. 115 (2018) 2114–2119.
[3] J. Wang, B. Foxman, L. Mody, E.S. Snitkin, Network of microbial and antibiotic interactions drive colonization and infection with multidrug-resistant organisms, Proc. Natl. Acad. Sci. U.S.A. 114 (2017) 10467–10472.
[4] U. Obolski, J. Lourenco, C. Thompson, R. Thompson, A. Gori, S. Gupta, Vaccination can drive an increase in frequencies of antibiotic resistance among nonvaccine serotypes of *Streptococcus pneumoniae*, Proc. Natl. Acad. Sci. U.S.A. 115 (2018) 3102–3107.
[5] D.A. Talan, W.R. Mower, A. Krishnadasan, F.M. Abrahamian, F. Lovecchio, D.J. Karras, M.T. Steele, R.E. Rothman, R. Hoagland, G.J. Moran, Trimethoprim-sulfamethoxazole versus Placebo for uncomplicated skin abscess, New Engl. J. Med. 374 (2016) 444–453.
[6] G.G. Zhanel, C.K. Lawrence, H. Adam, F. Schweizer, S. Zelenitsky, M. Zhanel, P.R.S. Lagace-Wiens, A. Walkty, A. Denisuik, A. Golden, A.S. Gin, D.J. Hoban, J.P. Lynch III, J.A. Karlowsky, Imipenem-relebactam and meropenem-vaborbactam: two novel Carbapenem-β-Lactamase inhibitor combinations, Drugs 78 (2018) 65–98.
[7] S.T. Bo, Z.F. Xu, L. Yang, P. Cheng, R.X. Tan, R.H. Jiao, H.M. Ge, Structure and biosynthesis of mayamycin B, a new polyketide with antibacterial activity from *Streptomyces* sp. 120454, J. Antibiot. 71 (2018) 601–605.
[8] S. Dhillon, S. Meropenem/vaborbactam: a review in complicated urinary tract infections, Drugs 78 (2018) 1259–1270.
[9] H.M. Cheng, Y. Chang, L.W. Zhang, J.F. Luo, Z.C. Tu, X.Y. Lu, Q.W. Zhang, J.B. Lu, X.M. Ren, K. Ding, Identification and optimization of new dual inhibitors of B-Raf and Epidermal Growth Factor Receptor kinases for overcoming resistance against Vemurafenib, J. Med. Chem. 57 (2014) 2692–2703.
[10] Z.P. Xiao, X.D. Wang, P.F. Wang, Y. Zhou, J.W. Zhang, L. Zhang, J. Zhou, S.S. Zhou, H. Ouyang, X.Y. Lin, M. Mustapa, A. Reyinbaike, H.L. Zhu, Design, synthesis, and evaluation of novel fluoroquinolone-flavonoid hybrids as potent antibiotics against drug-resistant microorganisms, Eur. J. Med. Chem. 80 (2014) 92–100.
[11] L.X. Li, X.C. Huang, R.Z. Huang, S.H. Gou, Z.M. Wang, H.S. Wang, Pt(IV) prodrugs containing microtubule inhibitors displayed potent antitumor activity and ability to overcome cisplatin resistance, Eur. J. Med. Chem. 156 (2018) 666–679.
[12] M. Guo, D. Zuo, J. Zhang, L. Xing, W. Gou, F. Jiang, N. Jiang, D. Zhang, X. Zhai, Dual potent ALK and ROS1 inhibitors combating drug-resistant mutants: synthesis and biological evaluation of aminopyridine-containing diarylaminopyrimidine derivatives, Eur. J. Med. Chem. 158 (2018) 322–333.
[13] J.Z. Wang, C.L. Ma, J. Wang, H. Jo, B. Canturk, G. Fiorin, L.H. Pinto, R.A. Lamb, M.L. Klein, W.F. DeGrado, Discovery of novel dual inhibitors of the wild-type and the most prevalent drug-resistant mutant, S31N, of the M2 proton channel from influenza A virus, J. Med. Chem. 56 (2013) 2804–2812.
[14] G.S. Basarab, J.I. Manchester, S. Bist, P.A. Boriack-Sjodin, B. Dangel, R. Illingworth, B.A. Sherer, S. Sriram, M. Uria-Nickelsen, A.E. Eakin, Fragment-to-Hit-to-Lead discovery of a novel pyridylurea scaffold of ATP competitive dual targeting type II Topoisomerase inhibiting antibacterial agents, J. Med. Chem. 56 (2013) 8712–8735.
[15] Y.H. Huang, G.Q. Dong, H.Q. Li, N. Liu, W.N. Zhang, C.Q. Sheng, Discovery of Janus Kinase 2 (JAK2) and Histone Deacetylase (HDAC) dual inhibitors as a novel strategy for the combinational treatment of Leukemia and invasive fungal infections, J. Med. Chem. 61 (2018) 6056–6074.
[16] C.J. Menet, A dual inhibition, a better solution: development of a JAK1/TYK2 inhibitor, J. Med. Chem. 61 (2018) 8594–8596.
[17] R. Morphy, Z. Rankovic, Designed multiple ligands. An emerging drug discovery paradigm, J. Med. Chem. 48 (2005) 6523–6543.
[18] D.B. Wigley, G.J. Davies, E.J. Dodson, A. Maxwell, G. Dodson, Crystal structure of an *N*-terminal fragment of the DNA gyrase B protein, Nature 351 (1991) 624–629.
[19] C. Davies, R.J. Heath, S.W. White, C.O. Rock, The 1.8 Å crystal structure and active-site architecture of β-ketoacyl-acyl carrier protein synthase III (FabH) from *Escherichia coli*, Structure 8 (2000) 185–195.
[20] A. Sugino, N.R. Cozzarelli, The intrinsic ATPase of DNA gyrase, J. Biol. Chem. 255 (1980) 6299–6306.
[21] J.H. Morais Cabral, A.P. Jackson, C.V. Smith, N. Shikotra, A. Maxwell, R.C. Liddington, Crystal structure of the breakage-reunion domain of DNA gyrase, Nature 388 (1997) 903–906.
[22] J. Gore, Z. Bryant, M.D. Stone, M. Nollmann, N.R. Cozzarelli, C. Bustamante, Mechanochemical analysis of DNA gyrase using rotor bead tracking, Nature 439 (2006) 100–104.
[23] E.C. Engle, S.H. Manes, K. Drlica, Differential effects of antibiotics inhibiting gyrase, J. Bacteriol. 149 (1982) 92–98.
[24] N. Zidar, H. Macut, T. Tomasic, M. Brvar, S. Montalvao, P. Tammela, T. Solmajer, L.P. Masic, J. Ilas, D. Kikelj, *N*-Phenyl-4,5-dibromopyrrolamides and *N*-phenylindolamides as ATP competitive DNA Gyrase B inhibitors: design, synthesis, and evaluation, J. Med. Chem. 58 (2015) 6179–6194.
[25] Y. Morimoto, T. Baba, T. Sasaki, K. Hiramatsu, Apigenin as an anti-quinolone-

resistance antibiotic, Int. J. Antimicrob. Ag. 46 (2015) 666–673.
[26] K. Lai, P. Yadav, A. Kumar, A. Kumar, A.K. Paul, A.K. Design, synthesis, characterization, antimicrobial evaluation and molecular modeling studies of some dehydroacetic acid-chalcone-1,2,3-triazole hybrids, Bioorg. Chem. 77 (2018) 236–244.
[27] K.H. Xu, S.S. He, S.C. Chen, G.L. Qiu, J.B. Shi, X.H. Liu, X.Y. Wu, J. Zhang, W.J. Tang, Free radical rearrangement synthesis and microbiological evaluation of novel 2-sulfoether-4-quinolone scaffolds as potential antibacterial agents, Eur. J. Med. Chem. 154 (2018) 144–154.
[28] L. Han, S. Lobo, K.A. Reynolds, Characterization of β-ketoacyl-acyl carrier protein synthase III from *Streptomyces glaucescens* and its role in initiation of fatty acid biosynthesis, J. Bacteriol. 180 (1998) 4481–4486.
[29] S.S. Khandekar, D.R. Gentry, G.S. Van Aller, P. Warren, H. Xiang, C. Silverman, M.L. Doyle, P.A. Chambers, A.K. Konstantinidis, M. Brandt, R.A. Daines, J.T. Lonsdale, Identification, substrate specificity, and inhibition of the *Streptococcus pneumoniae* β-ketoacyl-acyl carrier protein synthase III (FabH), J. Biol. Chem. 276 (2001) 30024–30030.
[30] Y. Li, G. Florava, K.A. Reynolds, Alteration of the fatty acid profile of *Streptomyces coelicolor* by replacement of the initiation enzyme 3-ketoacyl acyl carrier protein synthase III (FabH), J. Bacteriol. 187 (2005) 3795–3799.
[31] J.W. Yao, D.F. Bruhn, M.W. Frank, R.E. Lee, C.O. Rock, Activation of exogenous fatty acids to acyl-acyl carrier protein cannot bypass FabI inhibition in *Neisseria*, J. Biol. Chem. 291 (2016) 171–181.
[32] X.C. Wei, H.W. Song, L. Yin, M.G. Rizzo, R. Sidhu, D.F. Covey, D.S. Ory, C.F. Semenkovich, Fatty acid synthesis configures the plasma membrane for inflammation in diabetes, Nature 539 (2016) 294–298.
[33] L.J. Song, F. Barona-Gomez, C. Corre, L.K. Xiang, D.W. Udwary, M.B. Austin, J.P. Noel, B.S. Moore, G.L. Challis, Type III polyketide synthase β-ketoacyl-ACP starter unit and ethylmalonyl-CoA extender unit selectivity discovered by *Streptomyces coelicolor* genome mining, J. Am. Chem. Soc. 128 (2006) 14754–14755.
[34] E. Carceller, M. Merlos, M. Giral, D. Balsa, C. Almansa, J. Bartroli, J. Garcia-Rafanell, J. Forn, [(3-Pyridylalkyl)piperidylidene]benzocycloheptapyridine derivatives as dual antagonists of PAF and Histamine, J. Med. Chem. 37 (1994) 2697–2703.
[35] X.M. Zhang, H. Guo, Z.S. Li, F.H. Song, W.M. Wang, H.Q. Dai, L.X. Zhang, J.G. Wang, Synthesis and evaluation of isatin-β- thiosemicarbazones as novel agents against antibiotic-resistant Gram-positive bacterial species, Eur. J. Med. Chem. 101 (2015) 419–430.
[36] C.S. Wu, C. Du, J. Gubbens, Y.H. Choi, G.P. Van Wezel, Metabolomics-driven discovery of a prenylated isatin antibiotic produced by *Streptomyces* species MBT28, J. Nat. Prod. 78 (2015) 2355–2363.
[37] X.J. Yan, Z.S. Lv, J. Wen, S.J. Zhao, Z. Xu, Synthesis and *in vitro* evaluation of novel substituted isatin-propylene-1*H*-1,2,3-triazole-4-methylene -moxifloxacin hybrids for their anti-mycobacterial activities, Eur. J. Med. Chem. 143 (2018) 899–904.
[38] R. Wang, X.Y. Yin, Y.H. Zhang, W.T. Yan, Design, synthesis and antimicrobial evaluation of propylene-tethered ciprofloxacin-isatin hybrids, Eur. J. Med. Chem. 156 (2018) 580–586.
[39] A. Plaper, M. Golob, I. Hafner, M. Oblak, T. Solmajer, R. Jerala, Characterization of quercetin binding site on DNA gyrase, Biochem. Bioph. Res. Co. 306 (2003) 530–536.
[40] T.P.T. Cushnie, A.J. Lamb, Antimicrobial activity of flavonoids, Int. J. Antimicrob. Ag. 26 (2005) 343–356.
[41] B. Suriyanarayanan, K. Shanmugam, R.S. Santhosh, Synthetic quercetin inhibits mycobacterial growth possibly by interacting with DNA gyrase, Rom. Biotech. Lett. 18 (2013) 8587–8593.
[42] T. Wu, X.X. Zang, M.Y. He, S.Y. Pan, X.Y. Xu, Structure-activity relationship of flavonoids on their anti-*Escherichia coli* activity and inhibition of DNA gyrase, J. Agric. Food Chem. 61 (2013) 8185–8190.
[43] P.D. Cotter, R.P. Ross, C. Hill, Bacteriocins – a viable alternative to antibiotics? Nat. Rev. Microbiol. 11 (2013) 95–105.
[44] Y. Luo, Y.S. Yang, J. Fu, H.L. Zhu, Novel FabH inhibitors: a patent and article literature review (2000–2012), Expert Opin. Ther. Pat. 22 (2012) 1325–1336.
[45] X.L. Wang, Y.B. Zhang, J.F. Tang, Y.S. Yang, R.Q. Chen, F. Zhang, H.L. Zhu, Design, synthesis and antibacterial activities of vanillic acylhydrazone derivatives as potential β-ketoacyl-acyl carrier protein synthase III (FabH) inhibitors, Eur. J. Med. Chem. 57 (2012) 373–382.
[46] Y. Li, C.P. Zhao, H.P. Ma, M.Y. Zhao, Y.R. Xue, X.M. Wang, H.L. Zhu, Design, synthesis and antimicrobial activities evaluation of Schiff base derived from secnidazole derivatives as potential FabH inhibitors, Bioorg. Med. Chem. 21 (2013) 3120–3126.
[47] Y. Zhou, Y. Luo, Y.S. Yang, L. Lu, H.L. Zhu, Study of acylhydrazone derivatives with deoxygenated seven-membered rings as potential β-ketoacyl-acyl carrier protein synthase III (FabH) inhibitors, MedChemComm 7 (2016) 1980–1987.
[48] S. Brinster, G. Lamberet, B. Staels, P. Trieu-Cuot, A. Gruss, C. Poyart, Type II fatty acid synthesis is not a suitable antibiotic target for Gram-positive pathogens, Nature 458 (2009) 83–86.
[49] A.A. Firsov, I.Y. Lubenko, M.V. Smirnova, E.N. Strukova, S.H. Zinner, Enrichment of fluoroquinolone-resistant *Staphylococcus aureus*: oscillating ciprofloxacin concentrations simulated at the upper and lower portions of the mutant selection window, Antimicrob. Agents Ch. 52 (2008) 1924–1928.